




Smart film of jackfruit seed starch as a potential indicator of fish freshness

Leandro Araújo da COSTA¹, Izaura Cirino Nogueira DIÓGENES¹, Marília de Albuquerque OLIVEIRA²,
Sádwa Fernandes RIBEIRO³, Roselayne Ferro FURTADO², Maria do Socorro Rocha BASTOS²,
Maria Aparecida Santiago SILVA¹, Selene Daiha BENEVIDES^{2*} 

Abstract

Smart film from jackfruit seeds containing anthocyanin extract has potential application as a freshness indicator of fish as they deteriorate, changing the color as a function of the product pH. The lower solubility percentage of the films was evidenced by the lower anthocyanin extract volume. The films presented mean water vapour permeability values of 3.034 g.mm/kPa.h.m². The starch/anthocyanin film (ST4.0:AN5.0) showed higher tensile strength, while ST2.4:AN5.0 and ST3.0:AN5.3 showed lower resistance. A small change in color in the films was evidenced after 48 hours, and fish (FF10) presented a blue color after 146 hours with a reduction in a* values. Shrimp (SF10) presented negative b* values and grayish color. The indicator film provides an alternative for a convenient, non-destructive and easy-to-view method, as well as informing consumers about the quality of the packaged product. The indicator function of the film was positive, suggesting the potential use of industry co-products in developing smart food freshness indicator packaging.

Keywords: intelligent packaging; co-products; polysaccharide; *Artocarpus heterophyllus*.

Practical Application: Jackfruit seed starch film with anthocyanin extract: indicator of fish freshness.

1 Introduction

Traditional packaging systems have certain limitations as to the indication of freshness and quality of the food packaged at the time of purchase, and it is often difficult to visualize whether or not the product is suitable for consumption. Experts predict smart packaging to be the future in food packaging solutions, since the increase in consumer demand for fresh food has consequently led to substantial growth in the development of packaging capable of providing food freshness information, enhancing storage, transport and distribution security (Ariyaratna et al., 2017; Liu et al., 2018). Smart packaging systems containing indicators are based on communicating information through direct visual changes, mainly alterations in color. Deterioration of packaged food can be detected by a color change on the label/packaging in response to microbial growth, microorganisms, moisture and gases like oxygen and ammonia (Ariyaratna et al., 2017). Based on the characteristic of the color change in relation to the acidic or basic media, pH colorimetric indicators have presented great potential for use in monitoring food freshness when relating the pH values with oxidation and microbial deterioration in fish (Huang et al., 2019; Aghaei et al., 2020), seafood (Wu et al., 2019; Mohammadlinejad et al., 2020), pork (Chen et al., 2019), and packaged foods in general, for example, pork, milk and seafood (Qin et al., 2019). While biogenic amines are currently found among the decomposing agents of meat products, volatile amines such as ammonia, dimethylamine (DMA) and trimethylamine (TMA), designated as total volatile basic nitrogen (TVB-N), are responsible for the typical taste and smell of fish at the beginning

of microbial decomposition (Wei et al., 2019). Due to the toxicity of these compounds, the production of amine indicator films offer advantages for fish and seafood consumers (Dudnyk et al., 2018; Aghaei et al., 2020). The sensory characteristics of foods may vary depending on the quality of the raw material or the duration and temperature of storage and they can be determined using instrumental devices as well as by the perception of color, tissue, taste and smell through human senses. However, human senses may not always produce precise results since the color change in food is identified subjectively (Ünal Şengör et al., 2019).

Food deterioration has been also monitored by pH changes and natural dyes extracted from plants, fruits and vegetables (e.g. curcumin, blueberries, grapes, carrots) have shown potential use as indicators in smart films (Liu et al., 2018; Luchese et al., 2018; Tirtashi et al., 2019). Anthocyanins, a class of natural water-soluble dyes, are responsible for a wide range of colors found in several plants (from violet to red). Depending on the plant from which it is extracted, several molecular structures of anthocyanins can be found presenting different numbers of methoxyl and hydroxyl groups that influence their stability and color variation with pH. Due to the biodegradability, water-solubility and color sensitivity to pH medium, anthocyanins from the *Jamun* fruit (*Syzygium cumini*) and mulberry skin extracts and other food waste, for instance, have been reported as pH indicator dyes (Ma et al., 2018; Balbinot-Alfaro et al., 2019; Talukder et al., 2020). The incorporation of such natural dyes in polysaccharide-based

Received 20 Feb., 2020

Accepted 15 Apr., 2020

¹Departamento de Química Orgânica e Inorgânica, Universidade Federal do Ceará – UFC, Fortaleza, CE, Brasil

²Laboratório de Embalagens, Embrapa Agroindústria Tropical, Fortaleza, CE, Brasil

³Departamento de Engenharia de Alimentos, Universidade Federal do Ceará – UFC, Fortaleza, CE, Brasil

*Corresponding author: selene.benevides@embrapa.br

films have produced reliable responses to pH variations making them a diagnostic tool to ensure the safety and quality of food at the time of purchase (Halász & Csóka, 2018; Kurek et al., 2018; Liu et al., 2018; Chen et al., 2019; Liang et al., 2019). Starch extracted from tapioca, yam, corn has been considered a promising agent as a film component for food packaging (Othman et al., 2019; Santoso et al., 2019; Song et al., 2019) as it offers advantages by being obtained from renewable sources, it is biodegradable, has a relatively low cost, and is generally easy to obtain (Chen et al., 2019; Luchese et al., 2018).

The starch extracted from jackfruit (*Artocarpus heterophyllus*) seeds presents about 22.10% to 38.34% of amylose, classified as a high amylose starch. Jackfruit seed starch has a significantly higher gelatinization temperature, higher gelatinization enthalpy, and lower breakdown viscosity compared to most starches. The chemical composition of jackfruit starch varies according to different origins: protein (0.09-3.68%), lipid (0.02-0.99%), and ash (0.03-0.99%) (Chen et al., 2016; Zhang et al., 2019; Kringel et al., 2020). Jackfruit is easily propagated in hot climates and the Northeast Region of Brazil is a large producer, reaching 100 fruits per year/tree each of which containing about 15 to 25% of seeds (Madruga et al., 2014) which makes them a sustainable source to produce polysaccharide-based biodegradable films.

This work presents the results obtained for a biodegradable polysaccharide-based film produced from starch extracted from jackfruit seeds incorporated with anthocyanin, a natural dye extracted from black grapes. The produced films were characterized, and the color changes as function of pH variations were investigated aiming to monitor the freshness of tilapia fish and shrimp.

2 Materials and methods

2.1 Chemicals

Tilapia fish (*Oreochromis niloticus*) and gray shrimp (*Farfantepenaeus brasiliensis*) were purchased fresh and clean at the Mucuripe Fish Market in Fortaleza (Ceará, Brazil) and transported in an icebox to the laboratory where the pH was measured. Samples of about 16 g were immediately placed in separate glass beakers, capped with the starch-based films and fastened with elastic alloy so that the films stayed about 10 cm from the food. The beakers were conditioned at $10\text{ °C} \pm 1\text{ °C}$ and room temperature ($30\text{ °C} \pm 2\text{ °C}$) for the analyses protocols. Jackfruit seeds (*Artocarpus heterophyllus* Lam.), for starch extracting, and Midnight Beauty® and Sable Seedless® black grapes, for anthocyanin extracting, were obtained in local markets in Baturité (Ceará, Brazil) and Fortaleza (Ceará, Brazil) cities, respectively. The seeds were kept frozen ($\sim 18\text{ °C}$) until the day of starch extracting. Sodium bisulfite (NaHSO_3) PA 58.3% SO_2 (Vetec) was used for the starch extraction, while ethanol PA (Synth) and hydrochloric acid PA 36.5% (Dinâmica Química Contemporânea Ltda.) were used for anthocyanin extraction. The glycerol used in preparing the films was PA 99.5% with 0.5% moisture (Dinâmica Química Contemporânea Ltda.).

2.2 Apparatus and methods

A digital micrometer (resolution: 0.001 mm Mitutoyo) was used for the determination of the thickness of the films. FT-IR spectra were obtained on an IR Tracer-100 spectrophotometer (Shimadzu). The starch and anthocyanin extract were analyzed in a KBr pellet ($4000\text{--}400\text{ cm}^{-1}$ range), with a resolution of 4 cm^{-1} , operating in the range of $4000\text{ to }400\text{ cm}^{-1}$, and diffuse reflectance infrared Fourier transformed spectroscopy (ATR-FTIR). Thermogravimetric analyzes (TGA) were performed in a Q50 (TA Instruments, New Castle, USA) in alumina crucible with a heating rate of 10 °C min^{-1} in a synthetic air atmosphere and a flow rate of 50 mL min^{-1} in the temperature range $25\text{--}800\text{ °C}$. The sample masses were 5.13 mg for starch and 4.5 mg for the film. The extracted starch and the film were also analyzed by differential scanning calorimetry (DSC) on Q20 equipment (TA Instruments, New Castle, USA). The starch and film mass samples were 7.8 and 7.3 mg, respectively. The assay temperature ranged from $-30\text{ to }400\text{ °C}$ with a heating rate of 10 °C/min in an air atmosphere with a constant flow of 50 mL min^{-1} . Tensile tests were performed in an EMIC DL-3000 Universal Testing Machine (Emic, São José dos Pinhais, Brazil) with a load cell of 100 N, initial separation of adhesion of 100 mm and traction speed of 12.5 mm min^{-1} . For these tests, films with dimensions $12\text{ mm} \times 100\text{ mm}$ were cut, packed in a desiccator with controlled temperature ($23 \pm 1\text{ °C}$) and moisture (50%) for 48 hours. The tests were performed with five replicates for each treatment. A portable Colorimeter (Konica Minolta CR-410) equipment was used for the analyses of the color changes. The water solubility of the films was determined according to Gontard et al. (1994), with minor modifications. The films were cut into 22 mm diameter discs and the dry mass was determined until constant weight after being kept for 24 hours in an oven at 70 °C . After weighing, the samples were immersed in 50 mL of distilled water in an Erlenmeyer flask, capped with foil and allowed to stir in a bath (Marconi, MA 095) at 76.2 rpm and 25 °C for 24 hours. The samples were taken out of the water and placed in an oven at 70 °C for 24 hours for drying and then weighing. The solubility in water was expressed in percentage in mass of the solubilized material. The analyses were performed in quadruplicate. Water vapor permeability (WVP) was determined by gravimetry following ASTM E96-00 (American Society for Testing and Materials, 2000).

The films were cut into discs with 30 mm diameter and fixed to the permeability cell with 2 mL of distilled water. Cells with the films were stored at 26 °C and 75% relative humidity in dry box (Nalgon) desiccator containing silica gel and weighed 8 times for 24 hours. The analyses were performed in quadruplicate for each treatment and the result expressed in $\text{g}\cdot\text{mm}/\text{kPa}\cdot\text{h}\cdot\text{m}^2$. Tukey tests were run in order to evaluate if the difference in the data obtained in triplicate/quadruplicate are statistically significant.

2.3 Starch and anthocyanin extractions

The seeds of jackfruit were peeled and washed with tap water to remove excess peels. They were then immersed in 0.2% (w/v) SO_2 sodium bisulfite solution for 30 minutes, then gradually mashed in a blender until the residues were fine. The dense and uniform paste was pressed into Nonwoven Fabric (NWF) over a common sieve until the entire starch was extracted. The obtained

starch suspension was decanted for 30 minutes at 25 °C, washed thoroughly with NaHSO₃ solution and centrifuged at 10,000 rpm for 10 minutes at 25 °C. The supernatant was discarded and the precipitated starch was subjected to oven drying with circulation and air renewal (Solab, SL 102) at 45 °C, then crushed in an analytical mill (Basic Mill, A11). The starch extracted from the jackfruit seeds showed a percentage yield of 9.03% with a moisture content of 4.7%.

The skins of black grapes were washed, macerated and allowed to soak with ethanol/water extracting solvent (70:30), pH 2, under refrigeration and protected from light for 48 hours. The extract was vacuum filtered and concentrated by rotavapor (Buchi R-215) at 40 °C, stored under refrigeration and protected from light. A 3% anthocyanin extract in ethanol:water-HCl 1.5 mol/L

solution was homogenized in a mechanical stirrer for 2 minutes and kept overnight under refrigeration (~10 °C). After filtration, the extract was analyzed in a spectrophotometer (Agilent Cary 60 UV-Vis) to read absorbance at 535 nm wavelength for anthocyanin. The results were expressed as mg/100 g of extract and the calculation was performed following the relation (absorbance x dilution factor/98.2) in which 98.2 is the molar extinction coefficient (ϵ) of cyanidin-3-glycoside, the main constituent of the extract (Niketic-Aleksic & Hrazdina, 1972). The concentration of total anthocyanin found in the grapes was 254.7 mg/100 g.

2.4 Preparation of the starch-based films

As a typical procedure, the solution of the starch extracted from the jackfruit was stirred for 24 hours at room temperature, enabling better homogenization and dissolution of the granules. After heated up to 95 °C for complete starch gelatinization, the temperature was lowered under stirring up to 50 °C when glycerol and anthocyanin were added followed by stirring for more 30 min. The film-forming solution was poured onto a Mylar® glass plate and spreaded out with a 1.6 mm-thick stainless steel bar, and maintained at 30 °C for 24 hours.

Several assays were carried out with different starch and anthocyanin amounts to define the best proportion to be used in the film formation by the casting method (Table 1).

Table 1. Values of theoretical and experimental proportions of starch/anthocyanin (ST:AN) for the film formulations.

	Theoretical		Experimental	
	starch	extract	starch (g)	extract (mL)
ST2.4:AN2.5	-1	-1	2.4	2.5
ST2.4:AN5.0	+1	-1	2.4	5.0
ST4.0:AN2.5	-1	+1	4.0	2.5
ST4.0:AN5.0	+1	+1	4.0	5.0
ST1.9:AN3.5	-1.41	0	1.87	3.5
ST4.1:AN3.5	+1.41	0	4.13	3.5
ST3.0:AN1.3	0	-1.41	3.0	1.73
ST3.0:AN5.3	0	+1.41	3.0	5.27
ST3.0:AN3.5	0	0	3.0	3.5
ST3.0:AN3.5	0	0	3.0	3.5
ST3.0:AN3.5	0	0	3.0	3.5

ST = starch; AN = anthocyanin extract.

3 Results and discussion

The film-forming solutions containing different percentages (Table 1) of jackfruit starch and anthocyanin (ST/AN) were left to dry on glass plates following a simple casting procedure, as illustrated in Figure 1.

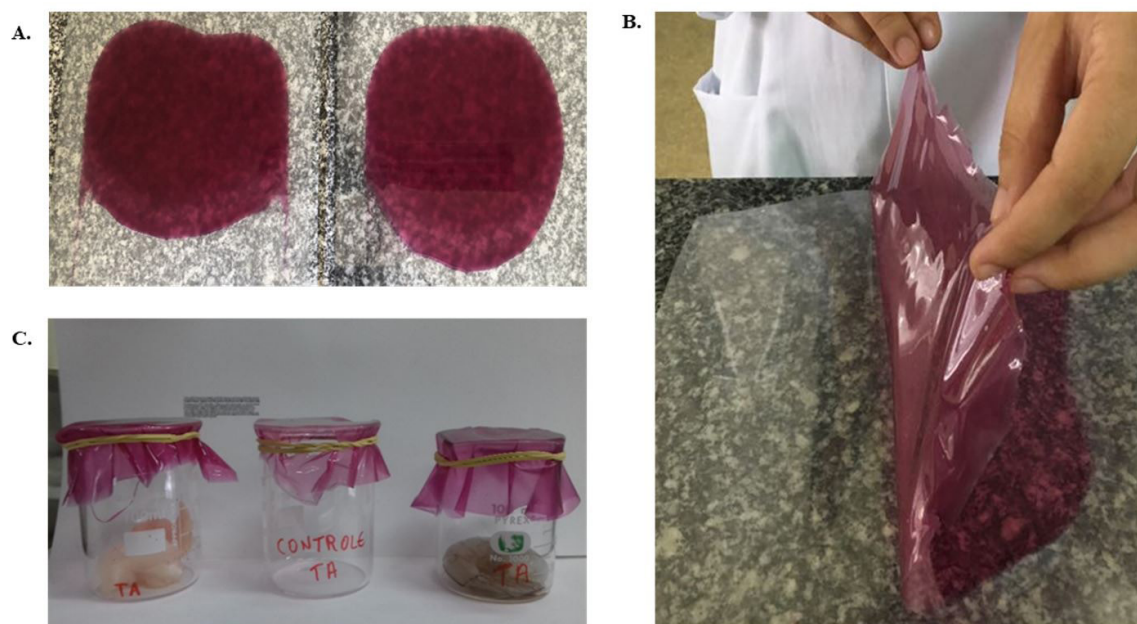


Figure 1. Films of the starch of jackfruit seed with anthocyanin (ST/AN). (A) film-forming solution drying on the glass plate; (B) film being removed from the plate showing the plastic-like aspect and (C) application of the films on beakers with fish and shrimp samples at room temperature (TA). A control beaker is shown in the center for comparison. Source: Selene Daiha Benevides.

After about 24h, the films presented a plastic-like aspect as can be ascertained from Figure 1B. It is important to note that the interaction with the starch did not promote the discoloration of the anthocyanins. Figure 1C shows the films placed on beakers containing fish and shrimp samples. All samples studied in this work present constant glycerol amount of 25% in relation to the total starch mass.

The thickness values of the ST/AN films presented a direct relation with the starch concentration ranging from 0.058 mm for the lower limit of starch (ST1.9:AN3.5) to 0.098 mm for the highest starch concentration (ST4.1:AN3.5). Table 2 presents the values of thickness (in mm) for different ratios of starch mass (in g) to anthocyanin volume (in mL).

While the thickness of the studied films presented a direct relation with the starch concentration, the solubility in water shown to be strongly dependent on the amount of anthocyanin, presenting solubilities going from 2.09% to 55.11% for the compositions ST3.0:AN1.3 and ST4.0:AN5.0 (Table 2), respectively. Such result is indeed expected due to the presence of hydroxyl groups in anthocyanin that favors the interaction with the water molecules through hydrogen bonds. High values of solubility, however, not only detrimentally affect the mechanical and barrier properties³³ of the film but also decrease its stability because of the inherent facility of dissolution. Similar values of water vapor permeability (WVP) were determined for all the samples as can be seen in Table 2 where an average value of $3.034 \text{ g.mm/kPa.h.m}^2 \pm 0.444$ can be found.

While the thickness of the studied films presented a direct relation with the starch concentration, the solubility in water shown to be strongly dependent on the amount of anthocyanin, presenting solubilities going from 2.09% to 55.11% for the compositions ST3.0:AN1.3 and ST4.0:AN5.0 (Table 2), respectively. Such result is indeed expected due to the presence of hydroxyl groups in anthocyanin that favors the interaction with the water molecules through hydrogen bonds. High values of solubility, however, not only detrimentally affect the mechanical and barrier properties (Azeredo et al., 2012) of the film but also decrease its stability because of the inherent facility of dissolution. Similar values of water vapor permeability (WVP) were determined for

all the samples as can be seen in Table 2 where an average value of $3.034 \text{ g.mm/kPa.h.m}^2 \pm 0.444$ can be found.

The lowest ($2.296 \text{ g.mm/kPa.h.m}^2$) and highest ($3.524 \text{ g.mm/kPa.h.m}^2$) WVP values were observed for ST1.9:AN3.5 and ST4.1:AN3.5, which contains lower and higher starch concentrations, respectively. These values are below those found by Kechichian et al. (2010) (4.65 to $9.01 \text{ g.mm m}^{-2} \text{ d}^{-1} \text{ kPa}$) when evaluating biodegradable films based on cassava starch added with natural antimicrobial ingredients also prepared by casting. The lower the WVP value, the greater the film efficiency with respect to the moisture barrier. The availability of hydroxyl groups for interaction with water is directly related to the permeability of biodegradable films and the greater the availability, the higher the WVP value (Mali et al., 2006).

Figure 2 shows the infrared spectra of the samples highlighting the regions of the stretching vibrational modes of OH, CH and CO. The spectrum of glycerol is also included for comparison purposes.

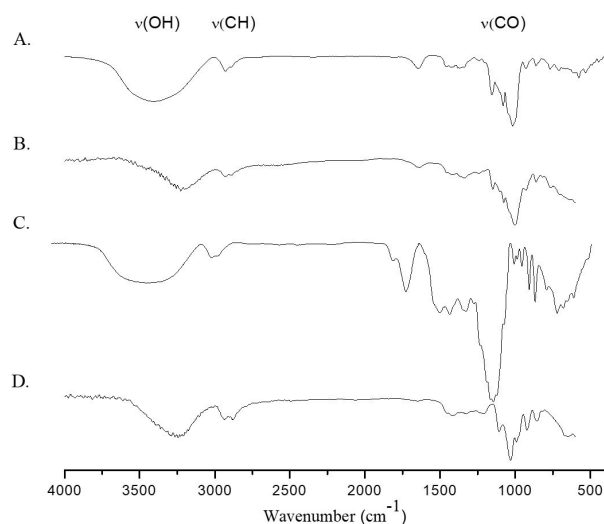


Figure 2. FTIR spectra of (A) starch, (B) ST4.0:AN5.0 film, (C) anthocyanin and (D) glycerol, highlighting the regions of the stretching vibrational modes of OH, CH and CO.

Table 2. Thickness, solubility, water vapor permeability (WVP), tensile strength and elongation at break of the ST/AN films.

Ratio (m/v)	Thickness (mm)	Solubility (%)	WVP (g.mm/kPa.h.m^2)	Tensile strength (MPa)	Elongation at break (%)
ST1.9:AN3.5	0.058 ± 0.003^b	52.18 ± 3.09^c	2.296 ± 0.203^b	4.35 ± 0.37^b	33.48 ± 0.29^{cd}
ST2.4:AN2.5	0.077 ± 0.003^f	5.62 ± 0.83^{cf}	2.817 ± 0.152^{cd}	6.14 ± 0.25^{bc}	23.38 ± 4.26^{ac}
ST2.4:AN5.0	0.066 ± 0.002^{de}	35.18 ± 3.31^d	2.737 ± 0.189^{abd}	5.88 ± 0.74^{bc}	26.97 ± 5.38^{cd}
ST3.0:AN1.3	0.073 ± 0.005^{cdf}	2.09 ± 1.49^f	3.088 ± 0.041^{cde}	6.52 ± 0.33^{ac}	13.33 ± 3.29^a
ST3.0:AN3.5	0.068 ± 0.001^{cde}	9.93 ± 1.31^e	3.119 ± 0.132^{cde}	6.17 ± 0.23^{bc}	35.39 ± 7.77^{bd}
ST3.0:AN3.5	0.068 ± 0.002^{cde}	4.86 ± 2.96^{cf}	3.263 ± 0.136^{ab}	6.14 ± 0.18^{bc}	35.12 ± 0.09^{bd}
ST3.0:AN3.5	0.063 ± 0.002^e	31.54 ± 2.94^d	2.473 ± 0.090^{ce}	7.38 ± 0.14^{ac}	45.11 ± 4.41^b
ST3.0:AN5.3	0.078 ± 0.005^f	7.61 ± 0.72^{cf}	3.478 ± 0.171^e	5.61 ± 1.95^{bc}	36.35 ± 3.13^{bd}
ST4.0:AN2.5	0.075 ± 0.002^{cf}	25.34 ± 0.17^b	3.376 ± 0.077^e	6.68 ± 0.47^{ac}	30.91 ± 2.09^{cd}
ST4.0:AN5.0	0.080 ± 0.001^f	55.11 ± 1.94^c	3.466 ± 0.238^e	8.16 ± 0.09^a	37.54 ± 3.09^{bd}
ST4.1:AN3.5	0.098 ± 0.002^a	42.43 ± 0.53^a	3.524 ± 0.160^e	6.73 ± 0.17^{ac}	29.32 ± 2.93^{cd}

ST = starch; AN = anthocyanin extract; m = mass in grams; v = volume in mL. Average of three values with standard deviation, same letter in the line indicates that there is no significant difference between the means by Tukey test ($p < 0.05$).

The vibrational spectra of all samples present a broad band at around 3200 cm^{-1} , assigned to the stretching vibrational mode (ν) of the OH bond of water and hydroxyl groups, and two weak sharp bands at around 2900 cm^{-1} , ascribed to the axial deformation (δ) of the CH_2 groups. The band at 1456 cm^{-1} in the spectrum of the starch sample, Figure 2A, is assigned to the in-plane bending vibration of OH bond typically seen in starch samples (Arik Kibar & Us, 2014; O'Connor, 1972). The region from 1200 to 900 cm^{-1} presents the characteristic starch bands (Figure 2A and B) assigned to the stretching vibrations of the CO bond in COH and COC groups (Chen et al., 2006; O'Connor, 1972). The spectrum of the anthocyanin extract, Figure 2C, presents a strong and relatively large band at around 1060 cm^{-1} assigned to the deformation of the CH bonds of the aromatic rings. The stretching vibration of the C=C bonds of the aromatic rings of the anthocyanin are observed at 1636 and 1405 cm^{-1} while the angular deformations of the CO bonds of the phenol moieties are seen at 1419 and 1340 cm^{-1} . The observation of the bands assigned to the stretching vibrations of the OH, CH and CO bonds in the spectrum of the ST/AN film, Figure 2B, indicates the presence of both the starch and anthocyanin starting materials.

The thermal decomposition of the ST/AN film was studied by temperature-dependent mass change (TG) and differential scanning calorimetry (DSC) techniques. The obtained thermograms are shown in Figure 3.

As can be ascertained from Figure 3A, the first event is observed at $66\text{ }^\circ\text{C}$ referring to the moisture loss of the starch (water loss of about 5%) being consistent with the moisture of the starch. The second event occurs at $308\text{ }^\circ\text{C}$ corresponding to a mass loss of 43.33% related to the polymer, and the third and last event occurs at $491\text{ }^\circ\text{C}$ with the mass loss of 96.13%, suggesting depolymerization of the backbone (Mukurumbira et al., 2017). Above $300\text{ }^\circ\text{C}$, the starch sample undergoes a series of irreversible changes associated starting with a structural alteration that leads the polymer to pyrodextrin (Han et al., 2018). For the ST/AN film, the first event, which is ascribed to moisture loss, occurs at $52\text{ }^\circ\text{C}$ corresponding to 1.69% of mass loss. The shoulder observed at $158\text{ }^\circ\text{C}$ is assigned (Flaker et al., 2010) to the degradation of glycerol. The second event is marked by a mass loss (19.60%) relative to anthocyanin at $205\text{ }^\circ\text{C}$, followed by polymer decomposition with about 51.68% of mass loss.

Two other well-defined events are observed at 461 and $496\text{ }^\circ\text{C}$ being assigned to the depolymerization of the starch backbone and the formation of β - (1-6) anhydrous D-glucopyranose (levoglycoside), 2-furaldehyde (furfural), among other low molar mass products (Aggarwal, & Dollimore, 1998). The mass changes for the two samples are completed at $510\text{ }^\circ\text{C}$ when the curve exhibits a constant range.

From the profiles of the DSC curves, Figure 3B, the melting temperature of the starch is observed at $105\text{ }^\circ\text{C}$. Upon incorporation of anthocyanin and glycerol for the film formation (red curve) this process is observed at $99\text{ }^\circ\text{C}$. Two other events are observed at 162.97 and at $207.41\text{ }^\circ\text{C}$ for the ST/AN film (black curve) being assigned to the melting of anthocyanin and starch, respectively.

3.1 Mechanical tests

It was possible to obtain values of the maximum tensile strength using the tensile test and percentage of elongation at break for all films prepared in the central composite rotational design (CCRD), according to Table 2.

The films generally had low tensile strength. However, in analyzing the starch:anthocyanin (ST:AN) ratios, it was observed that there was lower tensile strength in the lower starch concentration (ST1.9:AN3.5), which was already expected due to its lower thickness. The ST4.0:AN5.0 film showed higher tensile strength, and the ST2.4:AN5.0 and ST3.0:AN5.3 films presented lower resistance when compared to the others, and could have occurred due to the higher anthocyanin concentrations of 8.3% and 8.9%, respectively, relative to the starch concentration. A greater amount of anthocyanin may have clustered between the starch chains and decreased their strength. Halász & Csóka (2018) observed that the interaction between chitosan and chokeberry extract leads to low mobility of the polymer chain, a behavior reflected in the lower tensile strength values. The anthocyanin concentration had little effect on the elongation of the films, since the standard deviation was very high (values not shown), except for ST3.0:AN1.3 with a value of 14.84%. The elongation values at break found in the literature are very diverse, depending on the preparation conditions of the film (Ferreira et al., 2014; Kurek et al., 2018). The decrease in breaking elongation can be attributed to the formation of polyphenolic crystals accessible in the polymer matrix without being chemically bonded, and thus

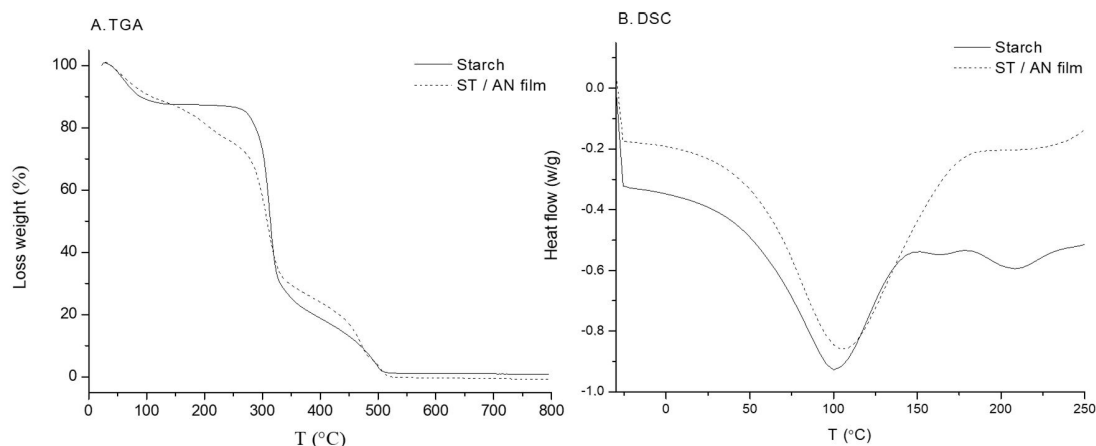


Figure 3. (A) TG and (B) DSC curves for jackfruit seed starch (—) and ST4.0:AN5.0 films (---).

the flexibility of the film is reduced. Similar results were reported by Pastor et al. (2013) and Siripatrawan & Vitthayakitti (2016). The authors found that the elongation decreased with increasing concentration of the propolis extract in the chitosan film.

3.2 Color change analysis of smart films

The evaluation of the film's color change occurred by exposing the film in different beakers with fish (FF) and shrimp (SF) samples, according to Figure 4. These foods release volatile amines (TVB-N) at the beginning of their microbial degradation, making it easier to see the color change of the film as a function of pH. The film selected for application in fish samples was ST4.0:AN5.0 because it presented better visual appearance (more homogeneous and without bubbles), greater thickness and greater mechanical resistance. Figure 4A shows fish samples stored at room temperature (30 °C) for 3 days. No color change was seen in the films in the first 7 hours.

After 24 hours, the fish sample film (FF30) showed a greenish color and the film covering the beaker with the shrimp (SF30) was slightly violet. At 3 days, the odor exhaled by the fish was already perceptible due to the deterioration process. The film that

covered the beaker with the fish was yellowish and the shrimp film was slightly green. The control film (CF30) showed no change in color. Figure 4B shows the samples during the 10 days of storage at 10 °C. The films that covered the beakers containing the fish presented a variation in color. No change in color of the films was seen in the first 24 hours of storage, but after 48 hours they started to show a slight color change and continued without much variation up to 72 hours. After 146 hours (6 days), the FF10 film presented bluish color and the SF10 was slightly blue.

After 240 hours (10 days) of storage, the FF10 film was green and the shrimp film was bluish. The CF10 film did not show a color change. At room temperature for 3 days, the initial fish pH (6.08) increased to 8.56 and the initial shrimp pH (6.80) increased to 7.76. For the refrigeration temperature test, the pH of the fish increased to 8.83 and the shrimp to 7.34. Fish deterioration increased pH due to decomposition of amino acids and urea. When the medium goes from neutral to alkaline, the fish becomes unsuitable for consumption. The fish film showed greater intensity of color change in both tests, indicative of greater release of volatile amines. The yellowish/green color of the films tested with the fish may have occurred due to the formation of chalcone (one of the anthocyanin structural forms). The blue color observed in the films tested with shrimp may be associated with the formation of the quinoidal base of anthocyanins.

Table 3. Luminosity L*, chroma a*, chroma b* of the films applied in fish (FF), shrimp (SF), and control (CF) samples stored at room (30 °C) and refrigerated (10 °C) temperatures.

Sample	L*	a*	b*
FF30	74.82 ± 0.00 ^a	2.13 ± 0.01 ^f	11.92 ± 0.02 ^a
SF30	67.47 ± 0.03 ^c	2.76 ± 0.04 ^e	-0.13 ± 0.01 ^b
CF30	66.25 ± 0.06 ^e	28.88 ± 0.02 ^a	-3.53 ± 0.02 ^d
FF10	66.50 ± 0.01 ^d	7.94 ± 0.03 ^d	-1.92 ± 0.01 ^c
SF10	68.89 ± 0.01 ^b	15.24 ± 0.04 ^c	-8.29 ± 0.02 ^f
CF10	64.35 ± 0.01 ^f	26.96 ± 0.06 ^b	-5.46 ± 0.03 ^e

Average of three values with standard deviation. Same letter in the line indicates that there is no significant difference between the means by Tukey test ($p < 0.05$).

L, a* and b* parameters (Table 3) were determined in order to evaluate the color variation in the films after the storage period when compared to the control film. Changes in these parameters indicate the relationship between color changes.

The films presented very close luminosity values with an average value of 68.03, indicating that they are lightly clear, with the exception of FF30. The a* parameter was evaluated due to incorporating anthocyanin to the films, where both CF10 and CF30 presented close values of 26.96 ± 0.06 and 28.88 ± 0.02, respectively, confirming red color. A reduction in the a* values

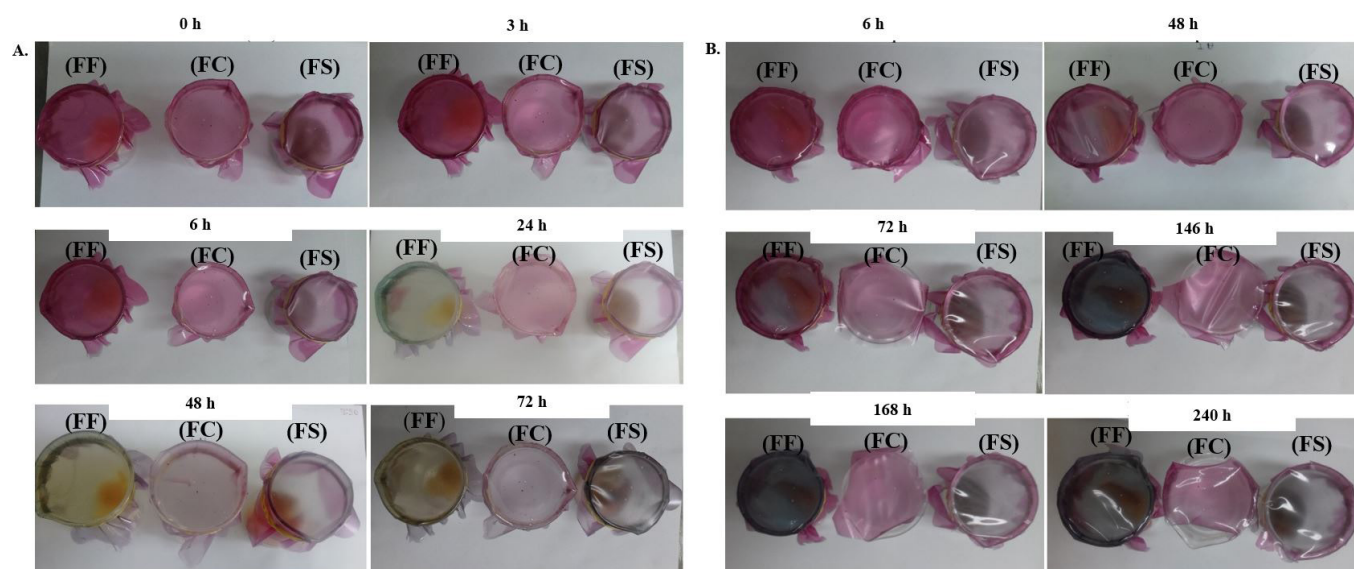


Figure 4. Visual appearance of jackfruit seed starch/anthocyanin films applied in beakers. Each photo contains fish (FF) on the left, control (FC) in the center and shrimp (FS) on the right stored at (A) room temperature (30 °C) and (B) refrigerated temperature (10 °C). Source: Selene Daiha Benevides.

was observed after the storage time with the fish. Another observation was related to the negative b^* values and close to zero, indicating slightly grayish films, except for FF30 which presented positive b^* values approaching yellow color.

The color change of the films can be justified by the release of volatile amines such as ammonia (NH_3), dimethylamine (DMA) and trimethylamine (TMA) over the course of fish deterioration. These substances which have pH above 7 react with the anthocyanins, causing the color change. Anthocyanins have a positive charge on their C ring in comparison to other flavonoids, which leads to different colors in response to various pH, with the most significant variation being in the basic region due to the lower stability of the molecules in that medium (Huang et al., 2019).

4 Conclusion

Smart films based on jackfruit seed starch with anthocyanins from grape skins added, both co-products from food processing industries, was developed, characterized and evaluated as a potential indicator of fish freshness. The results were found to be interesting from an industrial and commercial point of view, since both the materials used and the color change of the studied films can be adapted to different applications, helping the consumer when buying food. The color change occurred due to the release of TVB-N during the fish deterioration, altering the pH of the products which reacts with the anthocyanin. It was possible to establish a correlation between the color change and the freshness of the tested samples. However, further testing, including modifications of the starch used or polysaccharide blends, or even some type of reinforcement should be performed to verify improvements in mechanical characteristics. Different applications of the film in other foods and in adverse environmental conditions will favor its applicability as an smart pH-indicating film. One possibility of applying this film would be as a visual indicator in the form of a label indicating the food freshness when inserted into the product packaging.

References

- Aggarwal, P., & Dollimore, D. (1998). A thermal analysis investigation of partially hydrolyzed starch. *Thermochimica Acta*, 319(1-2), 17-25. [http://dx.doi.org/10.1016/S0040-6031\(98\)00355-4](http://dx.doi.org/10.1016/S0040-6031(98)00355-4).
- Aghaei, Z., Ghorani, B., Emadzadeh, B., Kadkhodae, R., & Tucker, N. (2020). Protein-based halochromic electrospun nanosensor for monitoring trout fish freshness. *Food Control*, 111, 107065. <http://dx.doi.org/10.1016/j.foodcont.2019.107065>.
- American Society for Testing and Materials – ASTM. (2000). *ASTM E96-00*. Philadelphia: ASTM.
- Arik Kibar, E. A., & Us, F. (2014). Evaluation of structural properties of cellulose ether-corn starch based biodegradable films. *International Journal of Polymeric Materials and Polymeric Biomaterials*, 63(7), 342-351. <http://dx.doi.org/10.1080/00914037.2013.845190>.
- Ariyaratna, I. R., Rajakaruna, R. M. P. I., & Karunaratne, D. N. (2017). The rise of inorganic nanomaterial implementation in food applications. *Food Control*, 77, 251-259. <http://dx.doi.org/10.1016/j.foodcont.2017.02.016>.
- Azeredo, H. M. C., Magalhães, U. S., Oliveira, S. A., Ribeiro, H. L., Brito, E. S., & De Moura, M. R. (2012). Tensile and water vapour properties of calcium-crosslinked alginate-cashew tree gum films. *International Journal of Food Science & Technology*, 47(4), 710-715. <http://dx.doi.org/10.1111/j.1365-2621.2011.02897.x>.
- Balbinot-Alfaro, E., Craveiro, D. V., Lima, K. O., Costa, H. L. G., Lopes, D. R., & Prentice, C. (2019). Intelligent Packaging with pH Indicator Potential. *Food Engineering Reviews*, 11(4), 235-244. <http://dx.doi.org/10.1007/s12393-019-09198-9>.
- Chen, H., Zhang, M., Bhandari, B., & Yang, C. (2019). Development of a novel colorimetric food package label for monitoring lean pork freshness. *Lebensmittel-Wissenschaft + Technologie*, 99, 43-49. <http://dx.doi.org/10.1016/j.lwt.2018.09.048>.
- Chen, J., Liang, Y., Li, X., Chen, L., & Xie, F. (2016). Supramolecular structure of jackfruit seed starch and its relationship with digestibility and physicochemical properties. *Carbohydrate Polymers*, 150, 269-277. <http://dx.doi.org/10.1016/j.carbpol.2016.05.030>. PMID:27312638.
- Chen, Y., Liu, S., & Wang, G. (2006). Kinetics and adsorption behavior of carboxymethyl starch on α -alumina in aqueous medium. *Journal of Colloid and Interface Science*, 303(2), 380-387. <http://dx.doi.org/10.1016/j.jcis.2006.08.011>. PMID:16996075.
- Dudnyk, I., Janeček, E.-R., Vaucher-Joset, J., & Stellacci, F. (2018). Edible sensors for meat and seafood freshness. *Sensors and Actuators B: Chemical*, 259, 1108-1112. <http://dx.doi.org/10.1016/j.snb.2017.12.057>.
- Ferreira, A. S., Nunes, C., Castro, A., Ferreira, P., & Coimbra, M. A. (2014). Influence of grape pomace extract incorporation on chitosan films properties. *Carbohydrate Polymers*, 113, 490-499. <http://dx.doi.org/10.1016/j.carbpol.2014.07.032>. PMID:25256511.
- Flaker, C. H. C., Ayala, G., Agudelo, A. C., & Vargas, R. A. (2010). Efecto del glicerol en las propiedades eléctricas, comportamiento de fase y permeabilidad al vapor de agua en películas basadas en almidón de papa. *Revista Colombiana de Física*, 42(3), 439.
- Gontard, N., Duchez, C., Cuq, J.-L., & Guilbert, S. (1994). Edible composite films of wheat gluten and lipids: water vapour permeability and other physical properties. *International Journal of Food Science & Technology*, 29(1), 39-50. <http://dx.doi.org/10.1111/j.1365-2621.1994.tb02045.x>.
- Halász, K., & Csóka, L. (2018). Black chokeberry (*Aronia melanocarpa*) pomace extract immobilized in chitosan for colorimetric pH indicator film application. *Food Packaging and Shelf Life*, 16, 185-193. <http://dx.doi.org/10.1016/j.fpsl.2018.03.002>.
- Han, X., Kang, J., Bai, Y., Xue, M., & Shi, Y.-C. (2018). Structure of pyroextrin in relation to its retrogradation properties. *Food Chemistry*, 242, 169-173. <http://dx.doi.org/10.1016/j.foodchem.2017.09.015>. PMID:29037674.
- Huang, S., Xiong, Y., Zou, Y., Dong, Q., Ding, F., Liu, X., & Li, H. (2019). A novel colorimetric indicator based on agar incorporated with *Arnebia euchroma* root extracts for monitoring fish freshness. *Food Hydrocolloids*, 90, 198-205. <http://dx.doi.org/10.1016/j.foodhyd.2018.12.009>.
- Kechichian, V., Ditchfield, C., Veiga-Santos, P., & Tadini, C. C. (2010). Natural antimicrobial ingredients incorporated in biodegradable films based on cassava starch. *Lebensmittel-Wissenschaft + Technologie*, 43(7), 1088-1094. <http://dx.doi.org/10.1016/j.lwt.2010.02.014>.
- Kringel, D. H., Dias, A. R. G., Zavareze, E. da R., & Gandra, E. A. (2020). Fruit wastes as promising sources of starch: extraction, properties, and applications dianini. *Stärke*, 72(3-4), 1900200. <http://dx.doi.org/10.1002/star.201900200>.
- Kurek, M., Garofulić, I. E., Bakić, M. T., Šćetar, M., Uzelac, V. D., & Galić, K. (2018). Development and evaluation of a novel antioxidant and pH indicator film based on chitosan and food waste sources of antioxidants. *Food Hydrocolloids*, 84, 238-246. <http://dx.doi.org/10.1016/j.foodhyd.2018.05.050>.

- Liang, T., Sun, G., Cao, L., Li, J., & Wang, L. (2019). A pH and NH₃ sensing intelligent film based on *Artemisia sphaerocephala* Krasch. gum and red cabbage anthocyanins anchored by carboxymethyl cellulose sodium added as a host complex. *Food Hydrocolloids*, 87, 858-868. <http://dx.doi.org/10.1016/j.foodhyd.2018.08.028>.
- Liu, J., Wang, H., Wang, P., Guo, M., Jiang, S., Li, X., & Jiang, S. (2018). Films based on κ -carrageenan incorporated with curcumin for freshness monitoring. *Food Hydrocolloids*, 83, 134-142. <http://dx.doi.org/10.1016/j.foodhyd.2018.05.012>.
- Luchese, C. L., Abdalla, V. F., Spada, J. C., & Tessaro, I. C. (2018). Evaluation of blueberry residue incorporated cassava starch film as pH indicator in different simulants and foodstuffs. *Food Hydrocolloids*, 82, 209-218. <http://dx.doi.org/10.1016/j.foodhyd.2018.04.010>.
- Ma, Q., Liang, T., Cao, L., & Wang, L. (2018). Intelligent poly (vinyl alcohol)-chitosan nanoparticles-mulberry extracts films capable of monitoring pH variations. *International Journal of Biological Macromolecules*, 108, 576-584. <http://dx.doi.org/10.1016/j.ijbiomac.2017.12.049>. PMID:29229241.
- Madruga, M. S., Albuquerque, F. S. M., Silva, I. R. A., Amaral, D. S., Magnani, M., & Queiroga, V. No. (2014). Chemical, morphological and functional properties of Brazilian jackfruit (*Artocarpus heterophyllus* L.) seeds starch. *Food Chemistry*, 143, 440-445. <http://dx.doi.org/10.1016/j.foodchem.2013.08.003>. PMID:24054264.
- Mali, S., Grossmann, M. V. E., García, M. A., Martino, M. N., & Zaritzky, N. E. (2006). Effects of controlled storage on thermal, mechanical and barrier properties of plasticized films from different starch sources. *Journal of Food Engineering*, 75(4), 453-460. <http://dx.doi.org/10.1016/j.jfoodeng.2005.04.031>.
- Mohammadalinejad, S., Almasi, H., & Moradi, M. (2020). Immobilization of *Echium amoenum* anthocyanins into bacterial cellulose film: a novel colorimetric pH indicator for freshness/spoilage monitoring of shrimp. *Food Control*, 113, 107169. <http://dx.doi.org/10.1016/j.foodcont.2020.107169>.
- Mukurumbira, A., Mariano, M., Dufresne, A., Mellem, J., & Amonsou, E. (2017). Microstructure, thermal properties and crystallinity of amadumbe starch nanocrystals. *International Journal of Biological Macromolecules*, 102, 241-247. <http://dx.doi.org/10.1016/j.ijbiomac.2017.04.030>. PMID:28400183.
- Niketic-Aleksic, G. K., & Hrazdina, G. (1972). Quantitative analysis of the anthocyanin content in grape juices and wines. *Lebensmittel-Wissenschaft+Technologie. Food Science and Technology*, 5(5), 163-165.
- O'Connor, R. T. (1972). *Instrumental analysis of cotton cellulose and modified cotton cellulose* (Fiber Science Series, No. 3, 490 p.). New York: Marcel Dekker.
- Othman, S. H., Majid, N. A., Tawakkal, O. S. M. A., Basha, R. K., Nordin, N., & Shapi'i, R. A. (2019). Tapioca starch films reinforced with microcrystalline cellulose for potential food packaging application. *Food Science and Technology*, 39(3), 605-612. <http://dx.doi.org/10.1590/fst.36017>.
- Pastor, C., Sanchez-Gonzalez, L., Chiralt, A., Chafer, M., & Gonzalez-Martinez, C. (2013). Physical and antioxidant properties of chitosan and methylcellulose based films containing resveratrol. *Food Hydrocolloids*, 30(1), 272-280. <http://dx.doi.org/10.1016/j.foodhyd.2012.05.026>.
- Qin, Y., Liu, Y., Yuan, L., Yong, H., & Liu, J. (2019). Preparation and characterization of antioxidant, antimicrobial and pH-sensitive films based on chitosan, silver nanoparticles and purple corn extract. *Food Hydrocolloids*, 96, 102-111. <http://dx.doi.org/10.1016/j.foodhyd.2019.05.017>.
- Santoso, B., Hazirah, R., Priyanto, G., Hermanto, & Sugito, (2019). Utilization of *Uncaria gambir* Roxb filtrate in the formation of bioactive edible films based on corn starch. *Food Science and Technology*, 39(4), 837-842. <http://dx.doi.org/10.1590/fst.06318>.
- Siripatrawan, U., & Vitchayakitti, W. (2016). Improving functional properties of chitosan films as active food packaging by incorporating with propolis. *Food Hydrocolloids*, 61, 695-702. <http://dx.doi.org/10.1016/j.foodhyd.2016.06.001>.
- Song, X., Cheng, L., & Tan, L. (2019). Edible iron yam and maize starch convenient food flavoring packaging films with lemon essential oil as plasticization. *Food Science and Technology*, 39(4), 971-979. <http://dx.doi.org/10.1590/fst.13118>.
- Talukder, S., Mendiratta, S. K., Kumar, R. R., Agrawal, R. K., Soni, A., Luke, A., & Chand, S. (2020). *Jamun* fruit (*Syzygium cumini*) skin extract based indicator for monitoring chicken patties quality during storage. *Journal of Food Science and Technology*, 57(2), 537-548. <http://dx.doi.org/10.1007/s13197-019-04084-y>. PMID:32116363.
- Tirtashi, F. E., Moradi, M., Tajik, H., Forough, M., Ezati, P., & Kuswandi, B. (2019). Cellulose/chitosan pH-responsive indicator incorporated with carrot anthocyanins for intelligent food packaging. *International Journal of Biological Macromolecules*, 136, 920-926. <http://dx.doi.org/10.1016/j.ijbiomac.2019.06.148>. PMID:31233799.
- Ünal Şengör, G. F., Balaban, M. O., Topaloğlu, B., Ayvaz, Z., Ceylan, Z., & Doğruyol, H. (2019). Color assessment by different techniques of gilthead seabream (*Sparus aurata*) during cold storage. *Food Science and Technology*, 39(3), 696-703. <http://dx.doi.org/10.1590/fst.02018>.
- Wei, P., Cao, J., Shen, X., & Li, C. (2019). The preservation effect and mechanism of gelatin on golden pompano (*Trachinotus blochii*) fillets during cold storage. *Food Science and Technology*, 39(Suppl. 2), 626-631. <http://dx.doi.org/10.1590/fst.28718>.
- Wu, C., Sun, J., Chen, M., Ge, Y., Ma, J., Hu, Y., Pang, J., & Yan, Z. (2019). Effect of oxidized chitin nanocrystals and curcumin into chitosan films for seafood freshness monitoring. *Food Hydrocolloids*, 95, 308-317. <http://dx.doi.org/10.1016/j.foodhyd.2019.04.047>.
- Zhang, Y., Li, B., Zhang, Y., Xu, F., Zhu, K., Li, S., Tan, L., Wu, G., & Dong, W. (2019). Effect of degree of polymerization of amylopectin on the gelatinization properties of jackfruit seed starch. *Food Chemistry*, 289, 152-159. <http://dx.doi.org/10.1016/j.foodchem.2019.03.033>. PMID:30955597.